Heteroepitaxial Diamond Growth

Fourth Quarterly Report
1 October 1994- 31 December 1994

Submitted to
Ballistic Missile Defense Organization
Innovative Science and Technology Office
Office of Naval Research
Program No. N00014-92-C-0081

Prepared by
Research Triangle Institute

83U-5294
September 1995

3040 Cornwallis Road • Post Office Box 12194 • Research Triangle Park, North Carolina 27709-2194 USA

REPORT DOCUMENT PAGE

Form Approved
OMB No 0704-0188

1. AGENCY USE ONLY *(Leave blank)*	2. REPORT DATE	3. REPORT TYPE AND DATES COVERED
	September 1995	Quarterly Report 1 October 1994 -- 31 December 1994

4. TITLE AND SUBTITLE

Heteroepitaxial Diamond Growth

5. FUNDING NUMBERS

N00014-92-C-0081

6. AUTHOR(S)

R. J. Markunas, R. A. Rudder, J. B. Posthill, R. E. Thomas, G. Hudson

7. PERFORMING ORGANIZATION NAME(S) AND ADDRESS(ES)

Research Triangle Institute
P. O. Box 12194
Research Triangle Park, NC 27709

8. PERFORMING ORGANIZATION REPORT NUMBER

83U-5294

9. SPONSORING/MONITORING AGENCY NAME(S) AND ADDRESSES(ES)

Office of Naval Research
800 N. Quincy Street
Arlington, VA 22217-5000

10. SPONSORING/MONITORING AGENCY REPORT NUMBER

11. SUPPLEMENTARY NOTES

12a. DISTRIBUTION/AVAILABILITY STATEMENT

Approved for public release; unlimited distribution

12b. DISTRIBUTION CODE

13. ABSTRACT

The combination of several processes, including 600°C homoepitaxial diamond growth with water/alcohol mixtures, has enabled the lift-off of a synthetic single-crystal C(100) plate of dimensions 2.0 mm × 0.5 mm × 17.5 μm. The essence of this lift-off (or cutting) technique involves forming a buried damaged layer in a diamond single-crystal substrate while still maintaining the crystalline surface suitable for homoepitaxy. After completion of epitaxy, the damaged region is graphitized and exposed to an etching environment from the edges, thereby enabling the synthetic crystal to lift-off.

14. SUBJECT TERMS

15. NUMBER OF PAGES

16. PRICE CODE

17. SECURITY CLASSIFICATION OF REPORT	18. SECURITY CLASSIFICATION OF THIS PAGE	19. SECURITY CLASSIFICATION OF ABSTRACT	20. LIMITATION OF ABSTRACT
UNCLASSIFIED	UNCLASSIFIED	UNCLASSIFIED	

TABLE OF CONTENTS

1.0 INTRODUCTION 1

2.0 SINGLE-CRYSTAL DIAMOND LIFT-OFF 2

3.0 PUBLICATIONS 3

Quarterly Report Fourth Quarter

1 October 1994- 31 December 1994

1.0 INTRODUCTION

This is the 1994 fourth quarterly report on the Heteroepitaxial Diamond Growth Program Contract No. N-00041-92-C-0081.

Research conducted in this quarter has predominantly focused on a method to fabricate a free-standing diamond single-crystal. In essence, this is a method to "cut" or "lift-off" a sheet of synthetic diamond single-crystal material. This is an essential technology that can be used in concert with our epitaxial joining and homoepitaxial diamond processes to make single-crystal diamond wafers. Additionally, we have extended our investigation of H-terminated diamond NEA surfaces and discerned details that enable such a surface to enable microstructural examination via SEM.

2.0 SINGLE-CRYSTAL DIAMOND LIFT-OFF

We have combined an implantation/anneal/contactless electrochemical etching technique devised at Naval Research Laboratories (NRL) by M. Marchywka, et al. with RTI's water/alcohol diamond homoepitaxial process to lift-off a single-crystal diamond plate of 17.5 μm thickness. The dimensions of this demonstration plate are: 20 mm × 0.5 mm. This is a multi-step process that is very sensitive to the details of each step, so this has been summarized in two manuscripts that are included in this report. No effort has been made to date to extend this lift-off technique to a larger area, however, this would be necessary to do to ensure its applicability to a large-area process. At this time, we foresee no intrinsic obstacle in doing this as all the component processes (implantation, annealing, etching, homoepitaxy) appear as if they will each individually scale as needed.

3.0 PUBLICATIONS

1. J. B. Posthill, D. P. Malta, T. P. Humphreys, G. C. Hudson, R. E. Thomas, R. A. Rudder, and R. J. Markunas, *Fabrication of a Free-Standing, Synthetic, Single-Crystal Diamond Plate Using Ion Implantation and Plasma-Enhanced Chemical Vapor Deposition*, Mater. Res. Soc. Symp. Proc., vol. 388 (1995) 299.

2. J. B. Posthill, D. P. Malta, T. P. Humphreys, G. C. Hudson, R. E. Thomas, R. A. Rudder, and R. J. Markunas, *Method of Fabricating a Free-Standing Diamond Single-Crystal Using Growth From the Vapor Phase*, submitted to: Diamond and Related Materials.

3. D. P. Malta, J. B. Posthill, T. P. Humphreys, and R. J. Markunas, *Interpretation of Secondary Electron Contrast from Negative Electron Affinity Diamond Surfaces,* Microscopy Society of America, Annual Meeting and Proceedings, Kansas City, MO (1995).

FABRICATION OF A FREE-STANDING, SYNTHETIC, SINGLE CRYSTAL DIAMOND PLATE USING ION IMPLANTATION AND PLASMA-ENHANCED CHEMICAL VAPOR DEPOSITION

J.B. POSTHILL, D.P. MALTA, T.P. HUMPHREYS, G.C. HUDSON, R.E. THOMAS, R.A. RUDDER, and R.J. MARKUNAS
Research Triangle Institute, Research Triangle Park, North Carolina 27709-2194

ABSTRACT

Using a specific combination of energetic and chemical processes we have grown homoepitaxial diamond on and lifted it off of a type Ia natural C(100) crystal. Before growth, the C(100) crystal is exposed to a self implant of 190keV energy and dose of 1E16 cm^{-2}. Low temperature (~600°C) homoepitaxial diamond growth conditions were used that are based on water-alcohol source chemistries. To achieve layer separation (lift-off), samples were annealed to a temperature sufficient to graphitize the buried implant-damaged region. Contactless electrochemical etching was found to remove the graphite, and a transparent synthetic (100) single crystal diamond plate of 17.5μm thickness was lifted off. This free-standing diamond single crystal plate was characterized and found to be comparable to homoepitaxial films grown on unimplanted single crystal diamond.

INTRODUCTION

Research efforts are underway world-wide in order to develop a low cost, single crystal diamond wafer that could be used for active electronic device fabrication or other technological purposes. One approach has been to develop a heteroepitaxial diamond technology using recent advances in thin film diamond deposition processes -- in particular various chemical vapor deposition (CVD) techniques. Different non-native substrates have been examined, with the greatest success being found with: cubic BN single crystals [1, 2], BeO single crystals [3], Ni single crystals [4], SiC single crystals [5] and Si single crystals [e.g., 6]. Efforts are underway to improve these heteroepitaxial diamond processes using these respective substrates in order to increase the quality and value of the diamond layers.

A second approach involves employing techniques to make a diamond single crystal template by careful positioning/bonding of multiple single crystal diamonds on a non-native substrate combined with homoepitaxial diamond growth in order to epitaxially join the diamonds. If successful, this could result in a diamond boule technology. Underlying this approach to making a single crystal diamond template, is prior research in this laboratory which demonstrated that epitaxial diamond could be grown laterally and vertically at comparable rates [7]. Specially patterned Si(100) wafers were made in order to hold small (< 100μm), similarly-faceted seed diamonds in an array of {111}-faceted pyramidal pits in the Si, and after growing ~240μm of CVD diamond on such a unique structure, a large-area mosaic diamond film was created [8]. Another version of this method involves starting with considerably larger diamond single crystals (2mm×2mm) that have had their edges and faces oriented and polished to (100) [9]. Two diamond crystals were soldered in close proximity to each other onto a Mo substrate and placed in a hot filament diamond CVD reactor for epitaxial joining. Reported most recently were results from this laboratory which utilized edge-oriented 3mm×3mm (100) diamonds that

Preprint from:
Mat. Res. Soc. Symp. Proc.,
vol. 388 (1995)
299-304.

were bonded to a Si substrate and then epitaxially joined [10]. In addition to these methods of making a large-area single crystal diamond template, a method must be developed to cut wafers that minimizes kerf losses.

We briefly describe our own demonstration of a method to "cut" a diamond single crystal combined with diamond homoepitaxial deposition based on plasma-enhanced CVD using water-alcohol mixtures in order to fabricate a free-standing, synthetic, single crystal diamond plate.

EXPERIMENTAL PROCEDURE AND RESULTS

Diamond Substrate Preparation

Type Ia (100) natural diamond single crystals were used for these proof-of-concept experiments. They were procured from the vendor with adequate polishing to enable good quality homoepitaxial diamond growth [11]. Different diamonds were implanted with C^{12} at 190keV commercially. Doses varying from 5E15 cm^{-2} to 5E16 cm^{-2} were examined, with the 1E16 cm^{-2} dose thus far representing the best combination of providing a surface to grow good quality homoepitaxial diamond on and enabling lift-off to be performed later. This will be the only sample from which results will be presented.

Diamond Growth

An rf-driven plasma enhanced CVD process that utilizes water and alcohol (ethanol) to grow the homoepitaxial films was used in this study. The use of alcohol/water mixtures for diamond growth was pioneered in this laboratory [12], and the development and details of this homoepitaxial diamond deposition process are reported elsewhere [13]. Briefly, the conditions of homoepitaxial diamond growth used were: Reactant flow was 18 sccm ethanol and 12 sccm water; Pressure = 1 Torr; Power (rf) ≅ 1.5kW; Growth temperature ≅ 600°C; Growth rate ≅ 0.5 $\mu m\text{-}hr^{-1}$. Diamond homoepitaxial growth was done on the implanted side of each diamond, with periodic interruption to inspect the progress of diamond homoepitaxy on the implanted substrates. Fig. 1 shows surface topographies as observed by scanning electron microscopy (SEM) after 1.6μm growth and 17.5μm growth on the same substrate (previously implanted with 1E16 cm^{-2} dose). The surfaces appear reasonably smooth, and the unidirectional "ridges" that are believed to be artifacts of the polishing process are no longer seen after the thickness of 17.5μm is reached. Epitaxy was verified using low energy electron diffraction (LEED) after 1.6μm growth. These results are very similar to those achieved upon diamond homoepitaxy on as-received diamond substrates using this growth process.

Separation Methods

The diamond was annealed in flowing N_2 at ~1000°C to graphitize the buried, implanted region, and the sides of the diamond, which had considerable growth on them, were ground to expose the edges of the buried graphitic region. Fig. 2 shows a side (cross-section) of the ground diamond with buried graphite layer and homoepitaxial film. Different methods were attempted to lift off the plate, which were (in the order they were employed): (1) heating in a CrO_3/H_2SO_4 solution (failed), (2) heated in flowing O_2 at up to 600°C (failed) [14], and contactless electrochemical etching in DI water (successful). This successful method was developed earlier by Marchywka, et al. [15]. One unique aspect of this etching process is that it occurs in a front which begins from a side of the wafer. When the buried graphitic region is progressively etched, that area no longer appears darkened to the unaided eye. Although not permitted to go to completion, it was clear when much of the original 2mm×2mm diamond had the buried graphitic

layer removed by etching. A portion of the layer was then pried off mechanically. The resulting 2mm×0.5mm×17.5μm single crystal diamond plate is shown in Fig. 3 with the RTI logo as a back drop. The transparent nature of the free standing diamond plate is evident.

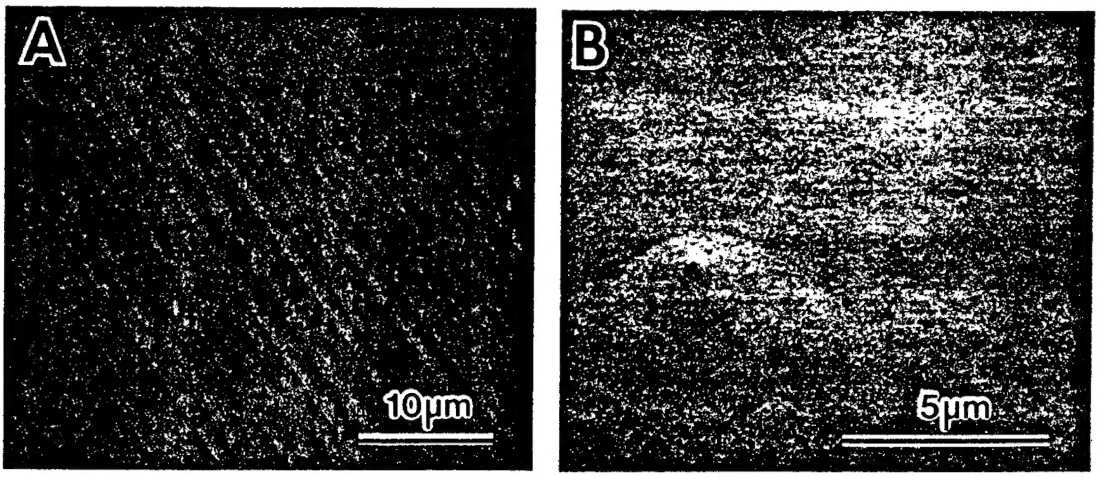

Fig. 1 SEM of homoepitaxial diamond grown on implanted diamond (100) crystal; (A) after 1.6μm growth and (B) after 17.5μm growth.

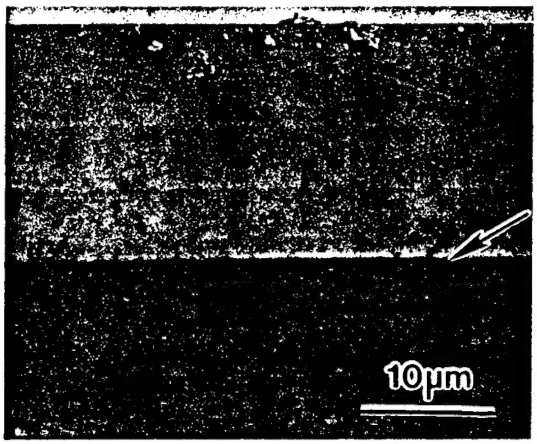

Fig. 2 SEM of ground edge after 17.5μm homoepitaxial diamond growth and 1000°C anneal. The location of the buried graphitic layer is delineated with an arrow.

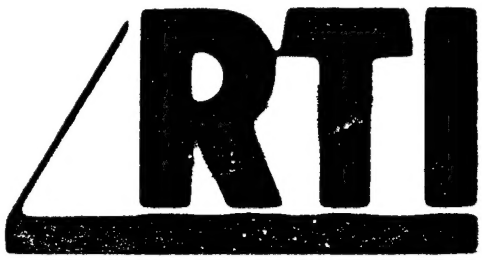

Fig. 3 Free-standing, synthetic, single crystal diamond plate which appears transparent over the RTI logo after contactless electrochemical etching of the buried graphitic region.

Characterization of Free-Standing Diamond Plate

The top surface of the lifted-off diamond plate was roughened; this had been earlier seen to be caused by the exposure of the diamond to flowing O_2 when heated. Additionally, the underside of the plate had some small pits. MicroRaman spectroscopy was performed on the region of the original diamond substrate on which implantation/growth/lift-off had occurred and on the lifted-off diamond plate. The spectra are shown in Fig. 4. Both had identical diamond LO phonon peak positions at 1332 cm^{-1} with full-width at half-maximum (FWHM) of 3.0 cm^{-1}. The background of the spectrum from the substrate is featureless, but the spectrum from the lifted-off plate shows a broadened peak at 2076 cm^{-1}. There is also broadband luminescence observed at increasing wave number. The 2076 cm^{-1} feature appears to be a luminescence peak (λ = 576nm; E = 2.153eV) that has been observed previously in nitrogen-containing CVD polycrystalline diamond using optical and electron excitation [16, 17]. It should be mentioned that no attempt was made to specifically remove or reduce the concentration of nitrogen in the liquid sources used for diamond growth in this study. Also, the first anneal in flowing N_2 may have contributed to the presence of this Raman feature. This point requires further investigation.

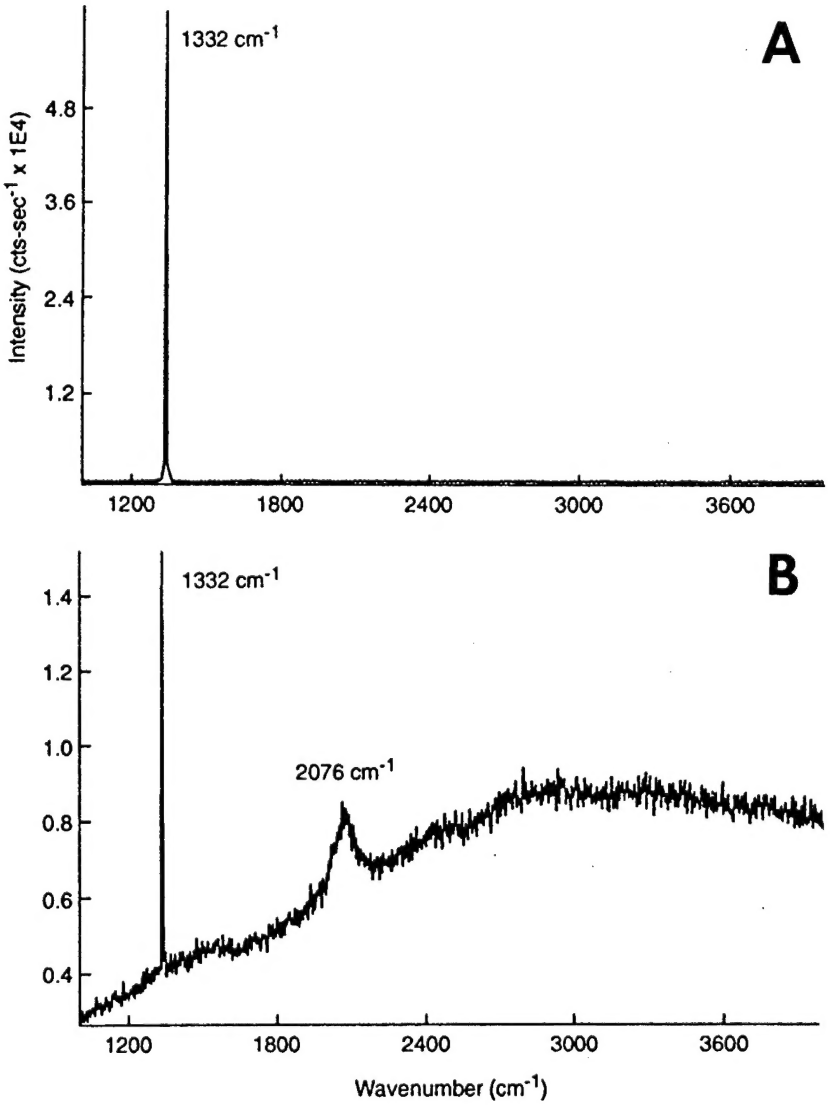

Fig. 4 MicroRaman spectra from; (A) natural type Ia substrate in region from which diamond plate was removed and (B) the lifted-off diamond plate as seen in Fig. 3.

The lifted-off diamond plate was then subjected to an oxidizing flame to assess the difference in defect densities by etch pit formation. This characterization technique has been used previously to delineate defects in natural single crystal diamonds, CVD polycrystalline diamond films [18], and homoepitaxial diamond. Fig. 5 shows an etch pit density (EPD) which is approximately 3×10^6 cm^{-2}. This is quite comparable to the EPD observed in other homoepitaxial diamond films grown in this laboratory [13].

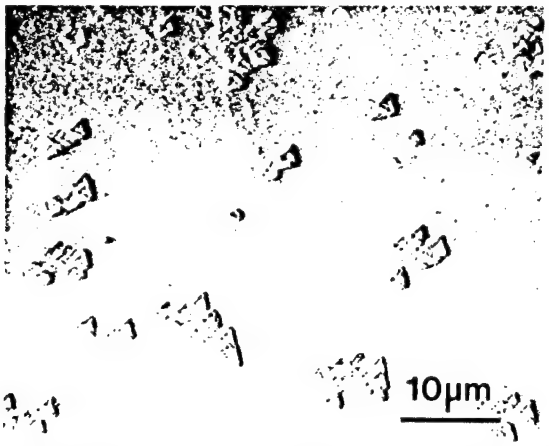

Fig. 5 SEM showing etch pit density on the top surface of the lifted-off diamond plate after 2 sec. exposure to an oxidizing flame. Density is ~ 3×10^6 cm^{-2}.

DISCUSSION AND SUMMARY

The separation (or lift off) of a single crystal homoepitaxial diamond film has been demonstrated at dimensions of ~ 2mm×0.5mm×17.5μm. This diamond plate could be handled and is transparent to the unaided eye. Both the surface topography and the defect density appear not to be compromised by the ion implantation required for lift-off. The ion implantation of carbon at 190keV is straight forward and can be done in a commercially-available, easily-accessible ion implanter. This multi-step process, as presented above, uses a relatively low temperature homoepitaxial diamond deposition process, but this may not be required. The water/alcohol growth chemistry is clearly compatible with good homoepitaxial diamond growth on ion implanted surfaces. The apparent presence of nitrogen in the lifted-off layer remains a concern, but the cause of this can be isolated and eliminated if it proves problematic. The future challenge of this technology is to ensure that the diamond lift-off process can be adequately scaled to larger area diamonds. If so, and when combined with a diamond boule technology [10], a synthetic diamond single crystal wafer fabrication process can be envisaged.

ACKNOWLEDGMENTS

We wish to thank M. Marchywka (Naval Research Laboratory) and R. Kessler (Univ. of North Carolina - Chapel Hill) for their scientific expertise and helpful discussions. The authors gratefully acknowledge support of this work by BMDO/IST through the Office of Naval Research (Contract No. N00014-92-C-0081).

REFERENCES

1. S. Koizumi, T. Murakami, T. Inuzuka, and K. Suzuki, Appl. Phys. Lett. **57**, 56 (1990).
2. L. Wang, P. Pirouz, A. Argoitia, J.S. Ma, and J.C. Angus, Appl. Phys. Lett. **63**, 1336 (1993).
3. A. Argoitia, J.C. Angus, L. Wang, X.I. Ning, and P. Pirouz, J. Appl. Phys. **73**, 4305 (1993).
4. W. Zhu, P.C. Yang, and J.T. Glass, Appl. Phys. Lett. **63**, 1640 (1993.
5. B.R. Stoner and J.T. Glass, Appl. Phys. Lett. **60**, 698 (1992).
6. X. Jiang, C.-P. Klages, R. Zachai, M. Hartweg, and H.-J. Fusser, Appl. Phys. Lett. **62**, 3438 (1993).
7. R.A. Rudder, J.B. Posthill, G.C. Hudson, D.P. Malta, R.E. Thomas, R.J. Markunas, T.P. Humphreys, and R.J. Nemanich, Proc. 2nd Intl. Conf. New Diamond Science and Technology, 1991 MRS Int. Conf. Proc., 425 (1991).
8. M.W. Geis, H.I. Smith, A. Argoita, J. Angus, G.-H.M. Ma, J.T. Glass, J. Butler, C.J. Robinson, and R. Pryor, Appl. Phys. Lett. **58**, 2485 (1991).
9. G. Janssen and L.J. Giling, Diamond and Related Materials, Diamond Films '94, (Il Ciocco, Italy, 1994) in press.
10. J.B. Posthill, D.P. Malta, G.C. Hudson, R.E. Thomas, T.P. Humphreys, R.C. Hendry, R.A. Rudder, and R.J. Markunas, submitted for publication - in review (1995).
11. Vendor for polished and oriented diamond single crystals: Harris Diamond Corp., Mount Arlington, New Jersey, USA; distributor for: Drukker International, Cuijik, The Netherlands.
12. R.A. Rudder, G.C. Hudson, J.B. Posthill, R.E. Thomas, R.C. Hendry, D.P. Malta, R.J. Markunas, T.P. Humphreys, and R.J. Nemanich, Appl. Phys. Lett. **60**, 329 (1992).
13. J.B. Posthill, T. George, D.P. Malta, T.P. Humphreys, R.A. Rudder, G.C. Hudson, R.E. Thomas, and R.J. Markunas, Proc. 51st Ann. Meeting Microsc. Soc. of America, edited by G.W. Bailey and C.L. Rieder (San Francisco Press, 1993) 1196.
14. N.R. Parikh, J.D. Hunn, E. McGucken, M.L. Swanson, C.W. White, R.A. Rudder, D.P. Malta, J.B. Posthill, and R.J. Markunas, Appl. Phys. Lett. **61**, 3124 (1992).
15. M. Marchywka, P.E. Pehrsson, D.J. Vestyck, Jr., and D. Moses, Appl. Phys. Lett. **63**, 3521 (1993).
16. L. Bergman, M.T. McClure, J.T. Glass, and R.J. Nemanich, J. Appl. Phys. **76**, 3020 (1994).
17. R.J. Graham and K.V. Ravi, Appl. Phys. Lett. **60**, 1310 (1992).
18. D.P. Malta, J.B. Posthill, R.A. Rudder, G.C. Hudson, and R.J. Markunas, J. Mater. Res. **8**, 1217 (1993).

Method of fabricating a free-standing diamond single crystal using growth from the vapor phase

J.B. Posthill, D.P. Malta, T.P. Humphreys, G.C. Hudson,

R.E. Thomas, R.A. Rudder, and R.J. Markunas

Research Triangle Institute, Research Triangle Park, North Carolina 27709-2194 USA

Abstract

By combining a low temperature (600°C) chemical vapor deposition process for homoepitaxial diamond and conventional ion implantation, we have made and lifted off a synthetic diamond single crystal plate. Before growth, a type Ia C(100) crystal was exposed to a self implant of 190keV energy and dose of 1×10^{16} cm^{-2}. Homoepitaxial diamond growth conditions were used that are based on water-alcohol source chemistries. To achieve layer separation ("lift-off"), samples were annealed to a temperature sufficient to graphitize the buried implant-damaged region. Contactless electrochemical etching was found to remove the graphite, and a transparent synthetic (100) single crystal diamond plate of 17.5μm thickness was lifted off. This free-standing diamond single crystal plate was characterized and found to be comparable to homoepitaxial films grown on unimplanted single crystal diamond.

Submitted to: Diamond and Related Materials

1. Introduction

Extensive research efforts are underway in order to develop a low cost, large-area, single crystal diamond wafer that could be used for active electronic device fabrication or other technological uses. One approach has been to develop a heteroepitaxial diamond technology using recent advances in thin film diamond deposition processes -- in particular various chemical vapor deposition (CVD) techniques. Different non-native substrates have been examined, with a degree of progress being found with: cubic BN single crystals [1, 2], BeO single crystals [3], Ni single crystals [4], SiC single crystals [5] and Si single crystals [e.g., 6]. Efforts are underway to improve these heteroepitaxial/oriented polycrystalline diamond processes using these respective substrates in order to increase the quality and utility of the diamond layers.

A second approach involves employing techniques to make a diamond single crystal template by careful positioning/bonding of multiple single crystal diamonds on a non-native substrate combined with homoepitaxial diamond growth in order to epitaxially join the diamonds. If successful, this could result in a diamond boule technology. Geis, et al. made specially patterned Si(100) wafers in order to hold small (< 100μm), similarly-faceted seed diamonds in an array of {111}-faceted pyramidal pits in the Si. After growing ~240μm of CVD diamond on this unique structure, the diamond seeds were epitaxially joined thereby creating a large-area mosaic diamond film [7]. A more recent demonstration of this approach using ~250μm cube-shaped diamonds that were arranged geometrically on a flat, non-native substrate were epitaxially joined to make a mosaic of ~ 1 cm^2 area [8]. Another version of this method involves starting with considerably larger diamond single crystals (2mm×2mm) that have had their edges and faces oriented and polished to (100). Two diamond crystals were soldered in close proximity to each other onto a Mo substrate and epitaxially joined using a hot filament

diamond CVD process [9]. Recently, results from this laboratory were reported which utilized edge-oriented 3mm×3mm×0.25mm (100) diamonds that were bonded to a Si substrate and then epitaxially joined using a low temperature (600°C) water-alcohol-based diamond growth process [10, 11].

In addition to these methods of making a large-area single crystal diamond template, a method needs to be developed to cut wafers that minimizes kerf losses and cost. One method of cutting a thin layer of diamond is via ion implantation; graphitization of the buried damaged region; and subsequent preferential etching of the buried, graphitic region. This is referred to as a "lift-off" technique. With the exception of using of an implantation/annealing step to form the buried, etchable layer, this concept is an interesting extension from the work of Yablonovitch, et al. where the preferential etching of a buried AlAs epitaxial layer enabled subsequent lift-off a thin GaAs epitaxial film [12]. Geis, et al. first formed a subsurface graphitic layer in diamond through ion implantation and annealing and then removed the top diamond layer with hot CrO_3/H_2SO_4 solution or molten KNO_3 [13]. Follow on work in this area included a lift-off demonstration on natural diamond single crystals which showed best results when implanting with oxygen at a very high energy (5 MeV) with a dose of 1×10^{18} cm^{-2} and etching the graphite in flowing oxygen at 550°C [14]. Thin, curled diamond sheets were removed in this manner, although some degree of buried graphitic layer etching could also be achieved upon exposure to hot CrO_3/H_2SO_4 solution. In an interesting extension to this concept, Tzeng, et al. grew homoepitaxial diamond on very high energy oxygen ion implanted diamond single crystals and then lifted off this (mainly) synthetic diamond sheet [15]. Another variant of this multi-step process was demonstrated at Oak Ridge National Laboratory where an excimer laser was used to pattern shapes into the homoepitaxial film such that these microcomponents were directly lifted

off upon etching the buried graphitic layer [16]. Unfortunately, these attempts at growing homoepitaxial diamond on the heavily implanted diamond substrates had severe surface topography problems as evidenced by optical microscopy. Although the source of these topographic irregularities is not known, it could potentially be due to the underlying implantation damage.

Concurrent with the above-described work, Marchywka, et al. showed that very high energy (MeV) implants may not be necessary for the successful implementation of diamond lift-off [17]. By using 175keV energy carbon implants at a considerably reduced dose (1×10^{16} cm^{-2}) combined with a novel contactless electrochemical etching process, lift-off of ultra thin diamond layers was achieved. Additionally, this Naval Research Laboratory effort has shown that it is possible to grow homoepitaxial diamond on such an implanted diamond prior to contactless electrochemical etching so as to lift-off the homoepitaxial layer from the substrate [18]. Their homoepitaxial diamond process was not yet optimized, but this demonstration of diamond epilayer lift-off using readily accessible ion implantation conditions is very promising and warrants further investigation.

Herein we describe our own diamond epilayer lift-off results from a diamond single crystal in the context of an optimized diamond homoepitaxial deposition based on plasma-enhanced CVD using water/alcohol mixtures. In particular, verifying that a low temperature, oxygen-containing diamond CVD process is compatible with high quality homoepitaxial diamond on a pre-implanted diamond substrate is required. Additionally, the effectiveness of the different buried graphitic layer etching techniques (wet chemical, flowing oxygen, and contactless electrochemical) with ion implantation conditions comparable to those used by

Marchywka, et al. [18] has been investigated. Detailed characterization results from the free-standing, synthetic, single crystal diamond plate are also presented.

2. Experimental Procedures

Type Ia (100) natural diamond single crystals were used for these experiments. They were procured from the vendor with adequate polishing to enable good quality homoepitaxial diamond growth [19]. Different diamonds were implanted with C^{12} at 190keV commercially. The diamonds were mechanically clamped to the implantation stage with no special provision for heat sinking, and the temperature during implantation was not measured. Three different doses; 1×10^{15} cm^{-2}, 1×10^{16} cm^{-2}, and 5×10^{16} cm^{-2} were implanted into different diamonds.

An rf-driven plasma enhanced CVD process that utilizes water and alcohol (ethanol) to grow the homoepitaxial films was used in this study. The use of alcohol/water mixtures for diamond growth was pioneered in this laboratory [20], and the details of this deposition process have been previously developed specifically to produce topographically smooth homoepitaxial diamond films reliably and reproducibly [21, 22]. The conditions of homoepitaxial diamond growth used were: Reactant flow was 18 sccm ethanol and 12 sccm water; Pressure = 1 Torr; Power (rf) $\cong$ 1.5kW; Growth temperature $\cong$ 600°C; Growth rate $\cong$ 0.5 $\mu m\text{-}hr^{-1}$. Diamond homoepitaxial growth was done on the implanted side of each diamond, with periodic interruption to inspect the progress of diamond homoepitaxy on the implanted substrates.

After diamond homoepitaxial growth, annealing in flowing N_2 at 1000°C to graphitize the buried, implanted region was carried out. The sides of the diamond, which had considerable growth on them, were ground to expose the edges of the buried graphitic region so that chemical attack could proceed. Grinding was achieved using an ambient temperature cast iron disc treated

with a diamond-particle-containing slurry. Three different methods were then sequentially attempted to etch the buried graphite layer and thereby lift-off the diamond homoepitaxial film, which were (in the order they were employed): (1) heating in a CrO_3/H_2SO_4 solution, (2) heating in flowing O_2 as high as 600°C, and (3) contactless electrochemical etching. Contactless electrochemical etching is described adequately elsewhere [17, 18] and was accomplished with house deionized (DI) water with graphite electrodes. A potential of 200 Vdc was used, and the current was found to be dependent on the condition of the graphite electrodes, which eroded in time. Periodically, they had to be replaced and the DI water refreshed, so as to keep the water from heating to a boil. No attempt was made to optimize this process for efficiency in this study.

Characterization was accomplished with optical examination, scanning electron microscopy (SEM), low energy electron diffraction (LEED), microRaman spectroscopy using the 514.5 nm line from an Ar^+ ion laser, and etch pit density (EPD) measurements upon exposing the homoepitaxial film to an oxidizing flame for 2 sec. This straight forward EPD technique for diamond is described elsewhere [23].

3. Experimental Results and Discussion

After C^{12} ion implantation at 190keV, the three crystals appeared differently. In particular, the diamonds implanted with doses 1×10^{16} cm^{-2} and 5×10^{16} cm^{-2} no longer appeared transparent to the unaided eye; they were opaque. The diamond implanted to the 1×10^{15} cm^{-2} dose still appeared optically transparent.

Homoepitaxial growth morphologies on all the implanted diamonds appeared characteristically good. Fig. 1 shows representative SEM micrographs of the surfaces, and a

series of micrographs after successive homoepitaxial layer thicknesses from the sample implanted to a dose of 1×10^{16} cm^{-2} is included to highlight this sample. This particular sample had the least smooth topography of the three. The growth surface still appears reasonably smooth, and the unidirectional "ridges" that are believed to be artifacts of the polishing process are no longer seen after the thickness of 17.5μm is reached. Epitaxy was verified for the 1×10^{16} cm^{-2} sample using low energy electron diffraction (LEED) after 1.6μm homoepitaxial diamond growth (Fig. 2). These results are very similar to those achieved upon diamond homoepitaxy on as-received diamond substrates using this growth process. It is inferred by the smooth morphologies seen for all the pre-implanted samples, that diamond epitaxy has been achieved on all substrates and at all thicknesses grown in this study.

Both the 1×10^{15} cm^{-2} and the 1×10^{16} cm^{-2} samples retained their pre-growth appearance to the unaided eye after growth, which were transparent and opaque, respectively. In contrast, the 5×10^{16} cm^{-2} sample became mainly transparent after growth, which was a dramatic change. Given the smooth topography and the absence of a darkened appearance, it is believed that the near-surface implanted portion of diamond had been etched by the diamond growth process that was used. This sample was no longer investigated as a candidate for lift-off; however, the excellent epitaxial surface did indicate a future potential for this process as a way to prepare or reclaim diamond surfaces for epitaxial growth [24]. By extension, the absence of an opaque appearance of the 1×10^{15} cm^{-2} sample led us to suspect that there was not a sufficiently damaged buried layer to enable the etching to occur for successful lift-off. Hence, the rest of our initial efforts focus on the 1×10^{16} cm^{-2} sample, and the balance of this contribution discusses these results.

After annealing and grinding the sides of the 1×10^{16} cm^{-2} homoepitaxial diamond, the ground diamond with buried graphite layer and homoepitaxial film is shown clearly in cross section SEM (Fig. 3). The different methods were then attempted to lift-off the homoepitaxial film. Heating in a CrO_3/H_2SO_4 solution did begin to attack the buried, damaged layer as evidenced by the groove observed in cross-section SEM (Fig. 4). However, the diamond still appeared opaque; indicating that this process was extremely slow and may be self-terminating. Upon attempting annealing the diamond in flowing oxygen, initially at 550°C for 6 hr., no change was seen at all. Further annealing at 600°C also had no effect on the presence of the dark appearance. At this point, the homoepitaxial diamond surface began to roughen, so going to higher temperatures in order to oxidize the buried graphitic layer was thought too likely to unacceptably damage the homoepitaxial diamond film.

Contactless electrochemical etching in DI water met with initial success. One unique aspect of this etching process is that it occurs in a front which begins from a side of the wafer. When the buried graphitic region is progressively etched, that area no longer appears darkened to the unaided eye. In this manner, the progress of etching could be assessed periodically. Although not optimized nor allowed to go to completion, most of the original 2mm×2mm diamond had the buried graphitic layer removed by etching. A portion of the layer was then pried off mechanically. The resulting 2mm×0.5mm×17.5μm single crystal diamond plate is shown in Fig. 5 with the RTI logo as a back drop. The transparent nature of the free standing diamond plate is evident, although there is a dull brownish tinge to the plate.

The top surface of the lifted-off diamond plate was roughened; this had been earlier seen to be caused by the exposure of the diamond to flowing O_2 when heated to 600°C.

Additionally, the underside of the plate had some very small pits; their origin is currently unknown (Fig. 6A). The now revealed surface of the bulk diamond showed remnants of initial scratch lines as well as the very small protrusions that appear to correlate with the small pits in the lifted-off single crystal plate (Fig. 6B). MicroRaman spectroscopy was performed on the region of the original diamond substrate on which implantation/growth/lift-off had occurred and on the lifted-off diamond plate. The spectra are shown in Fig. 7. Both had identical diamond LO phonon peak positions at 1332.0 cm^{-1} with full-width at half-maximum (FWHM) of 3.0 cm^{-1}. This indicates that the lifted off plate is strain-free and has a crystal quality comparable to the diamond substrate. The background of the spectrum from the substrate is featureless, but the spectrum from the lifted-off plate shows a broadened peak at 2076 cm^{-1}. There is also broadband luminescence observed at increasing wave number. The 2076 cm^{-1} feature appears to be a luminescence peak (λ = 576nm; E = 2.153eV) that has been observed previously in nitrogen-containing CVD polycrystalline diamond using Raman spectroscopy [25]. This feature has also been observed in cathodoluminescence studies of CVD epitaxial diamond [26, 27], and there appears to be a consensus in the literature to date that this peak is associated with a nitrogen-vacancy complex. The presence of nitrogen in the lifted-off plate is also consistent with the light dull brown color of the plate as observed to the eye. It should be mentioned that no attempt was made to specifically remove or reduce the concentration of nitrogen in the liquid sources used for diamond growth in this study. Also, the first anneal in flowing N_2 may have contributed to the presence of this Raman feature. This is an issue that may require further attention.

The lifted-off diamond plate was then subjected to an oxidizing flame to assess the difference in defect densities by etch pit formation. This characterization technique has been

used previously to delineate defects in natural single crystal diamonds, CVD polycrystalline diamond films [23], and homoepitaxial diamond. Fig. 8 shows an etch pit density (EPD) which is approximately 3×10^6 cm^{-2}. This is quite comparable to the EPD observed in other homoepitaxial diamond films grown on type Ia C(100) substrates in this laboratory, which have been in the 10^6 cm^{-2} density range [21, 22]. The fact that the EPD did not dramatically increase as a result of all the pre-growth diamond processing (in particular, ion implantation) and post-growth processing is an encouraging sign that this cutting process can be used to lift-off state-of-the-art single crystal diamond films for different technological applications.

Lifting off thin diamond single crystal plates can be combined with other developing technologies such as the aforementioned epitaxial joining of diamond single crystals to create a large-area diamond sheet [10,11]. The technology exists to handle, transfer, and bond sheets of single crystal diamond to other substrates such as Si. These proof-of-concept experiments show the direction towards a large-area, diamond single crystal substrate and boule manufacturing process.

4. Summary

Lift-off of a single crystal homoepitaxial diamond film has been demonstrated at dimensions of ~ 2mm×0.5mm×17.5μm. This resulting diamond plate could be handled and is transparent to the unaided eye. Both the surface topography and the defect density appear not to be compromised by the ion implantation required for lift-off when compared with other diamond homoepitaxial films grown in our laboratory on unimplanted diamond wafers. The ion implantation of carbon at 190keV at a moderate dose of 1×10^{16} cm^{-2} can easily be done in a commercially-available, easily-accessible ion implanter. This multi-step process, as presented

above, uses a relatively low temperature homoepitaxial diamond water/alcohol CVD process which is compatible with good homoepitaxial diamond growth on ion implanted diamond surfaces. One of the future challenges of this process is to ensure that the diamond lift-off can be adequately scaled to larger area diamond wafers.

Acknowledgements

We wish to thank M. Marchywka (Naval Research Laboratory) and R. Kessler (Univ. of North Carolina - Chapel Hill) for their scientific expertise and helpful discussions. The authors gratefully acknowledge support of this work by BMDO/IST through the Office of Naval Research (Contract No. N00014-92-C-0081).

References

1. S. Koizumi, T. Murakami, T. Inuzuka, and K. Suzuki, Appl. Phys. Lett. **57**, 56 (1990).
2. L. Wang, P. Pirouz, A. Argoitia, J.S. Ma, and J.C. Angus, Appl. Phys. Lett. **63**, 1336 (1993).
3. A. Argoitia, J.C. Angus, L. Wang, X.I. Ning, and P. Pirouz, J. Appl. Phys. **73**, 4305 (1993).
4. W. Zhu, P.C. Yang, and J.T. Glass, Appl. Phys. Lett. **63**, 1640 (1993.
5. B.R. Stoner and J.T. Glass, Appl. Phys. Lett. **60**, 698 (1992).
6. X. Jiang, C.-P. Klages, R. Zachai, M. Hartweg, and H.-J. Fusser, Appl. Phys. Lett. **62**, 3438 (1993).
7. M.W. Geis, H.I. Smith, A. Argoita, J. Angus, G.-H.M. Ma, J.T. Glass, J. Butler, C.J.

Robinson, and R. Pryor, Appl. Phys. Lett. **58**, 2485 (1991).

8. M.W. Geis, N.N. Efremow, R. Susalka, J.C. Twichell, K.A. Snail, C. Spiro, B. Sweeting, and S. Holly, Diamond and Related Materials, **4/1**, 76 (1994).

9. G.Janssen and L.J. Giling, Proc. 4th Intl. Conf. New Diamond Science and Technology, Eds. S. Saito, et al., (Kobe, Japan, 18-22 July 1994) 295.

10. J.B. Posthill, D.P. Malta, G.C. Hudson, R.E. Thomas, T.P. Humphreys, R.C. Hendry, R.A. Rudder, and R.J. Markunas, submitted for publication at: Thin Solid Films (1995).

11. D.P. Malta, J.B. Posthill, G.C. Hudson, R.E. Thomas, T.P. Humphreys, R.A. Rudder, and R.J. Markunas, Proc. 4th Intl. Symp. on Diamond Materials [The Electrochemical Society, Pennington, NJ] **95-4**, 509 (1995).

12. E. Yablonovitch, T. Gmitter, J.P. Harbison, and R. Bhat, Appl. Phys. Lett., **51**, 2222 (1987).

13. M.W. Geis, D.D. Rathman, and M. Rothschild, *Diamond Technology Initiative*, Arlington, VA, 12-13 July 1988.

14. N.R. Parikh, J.D. Hunn, E. McGucken, M.L. Swanson, C.W. White, R.A. Rudder, D.P. Malta, J.B. Posthill, and R.J. Markunas, Appl. Phys. Lett. **61**, 3124 (1992).

15. Y. Tzeng, J. Wei, J.T. Woo, and W. Lanford, Appl. Phys. Lett. **63**, 2216 (1993).

16. J.D. Hunn, S.P. Withrow, C.W. White, R.E. Clausing, L. Heatherly, and C.P. Christensen, Appl. Phys. Lett., **65**, 3072 (1994).

17. M. Marchywka, P.E. Pehrsson, S.C. Binari, and D. Moses, J. Electrochemical Soc. **140**, L19 (1993).

18. M. Marchywka, P.E. Pehrsson, D.J. Vestyck, Jr., and D. Moses, Appl. Phys. Lett. **63** 3521 (1993).

19. Vendor for polished and oriented diamond single crystals: Harris Diamond Corp., Mount Arlington, New Jersey, USA; distributor for: Drukker International, Cuijik, The Netherlands.

20. R.A. Rudder, G.C. Hudson, J.B. Posthill, R.E. Thomas, R.C. Hendry, D.P. Malta, R.J. Markunas, T.P. Humphreys, and R.J. Nemanich, Appl. Phys. Lett. **60**, 329 (1992).

21. J.B. Posthill, D.P. Malta, R.A. Rudder, G.C. Hudson, R.E. Thomas, R.J. Markunas, T.P. Humphreys, and R.J. Nemanich, Proc. 3rd Intl. Symp. on Diamond Materials [The Electrochemical Society, Pennington, NJ] **93-17**, 303 (1993).

22. J.B. Posthill, T. George, D.P. Malta, T.P. Humphreys, R.A. Rudder, G.C. Hudson, R.E. Thomas, and R.J. Markunas, Proc. 51st Ann. Meeting Microsc. Soc. of America, edited by G.W. Bailey and C.L. Rieder (San Francisco Press, 1993) 1196.

23. D.P. Malta, J.B. Posthill, R.A. Rudder, G.C. Hudson, and R.J. Markunas, J. Mater. Res. **8**, 1217 (1993).

24. T.P. Humphreys, J.B. Posthill, D.P. Malta, R.E. Thomas, R.A. Rudder, G.C. Hudson, and R.J. Markunas, Mater. Res. Soc. Symp. Proc., **339**, 51 (1994).

25. L. Bergman, M.T. McClure, J.T. Glass, and R.J. Nemanich, J. Appl. Phys. **76**, 3020 (1994).

26. R.J. Graham and K.V. Ravi, Appl. Phys. Lett. **60**, 1310 (1992).

27. S. Katsumata, Jpn. J. Appl. Phys., **31**, 3594 (1992).

Figure Captions

Fig. 1 SEM showing surface morphologies of homoepitaxial diamond grown on C^{12}, 190keV implanted C(100) Ia crystals; (A) Dose = 1×10^{15} cm^{-2} after 5.5μm growth, (B) Dose = 1×10^{16} cm^{-2} after 1.6μm growth, (C) Dose = 1×10^{16} cm^{-2} [continued] after 4.8μm total growth, (D) Dose = 1×10^{16} cm^{-2} [continued] after 9.2μm total growth, (E) Dose = 1×10^{16} cm^{-2} [continued] after 17.5μm total growth, and (F) Dose = 5×10^{16} cm^{-2} after 2μm growth.

Fig.2 Low energy electron diffraction (LEED) pattern taken after 1.6μm homoepitaxial diamond growth on ion implanted [C^{12}, 190keV, 1×10^{16} cm^{-2}] C(100) Ia crystal.

Fig. 3 SEM cross-section micrograph of ground edge after 17.5μm homoepitaxial diamond growth and 1000°C anneal. The location of the buried graphitic layer is delineated by the dark contrast.

Fig. 4 SEM cross-section micrograph showing groove beginning to form at the buried graphitic region after heating diamond sample in CrO_3/H_2SO_4 solution.

Fig. 5 Free-standing, synthetic, single crystal diamond plate which appears transparent over the RTI logo.

Fig. 6 SEM of diamond surfaces after contactless electrochemical etch and separation (lift-off); (A) underside of lifted-off single crystal diamond plate and (B) freshly exposed C(100) Ia substrate surface.

Fig. 7 MicroRaman spectra from; (A) C(100) Ia substrate in region from which diamond plate was removed and (B) lifted-off synthetic single crystal diamond plate.

Fig. 8 SEM showing EPD on the top surface of the lifted-off diamond plate after exposure to an oxidizing flame. Density is 3×10^{6} cm^{-2}.

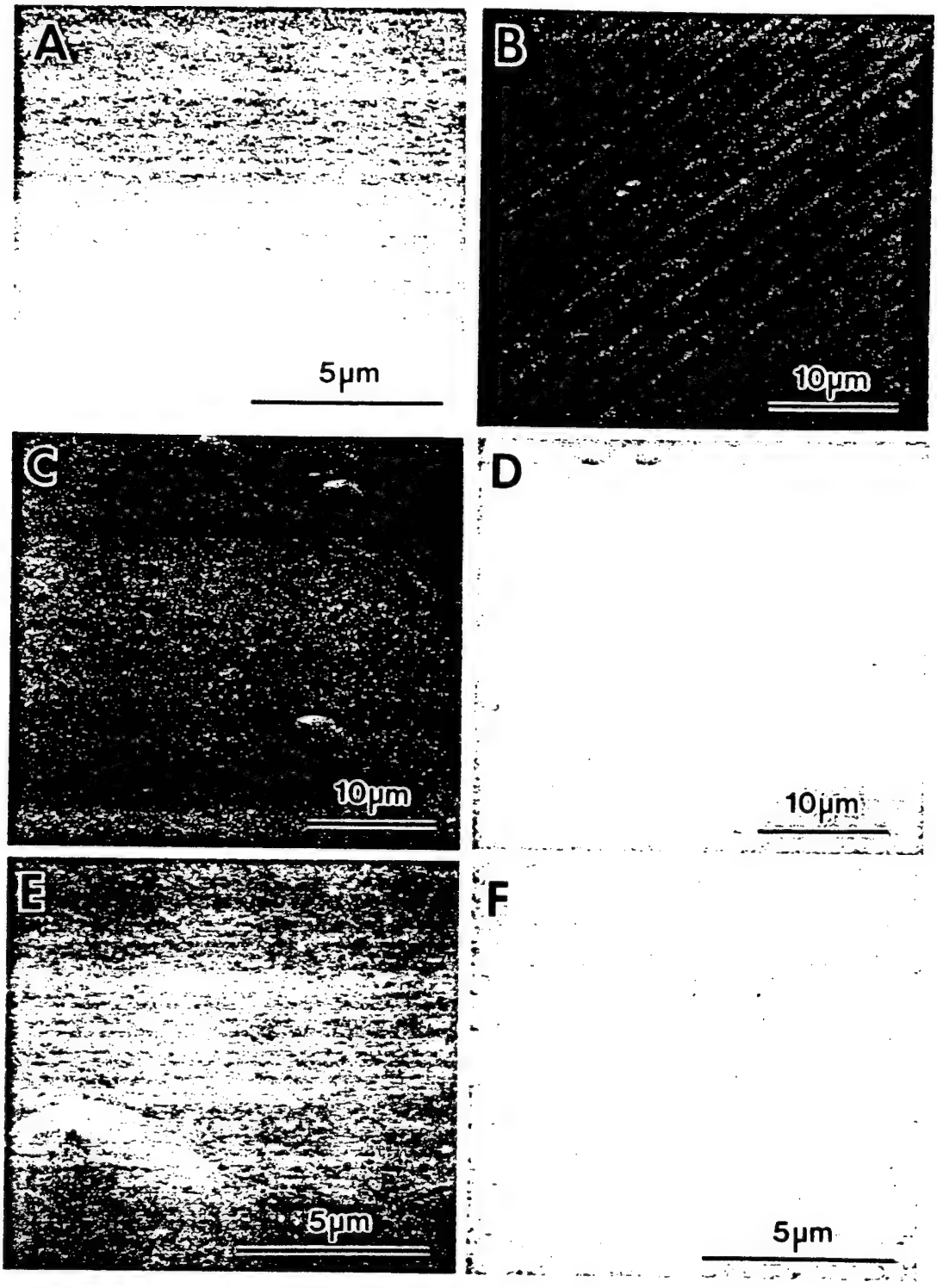

Fig. 1

Fig. 2

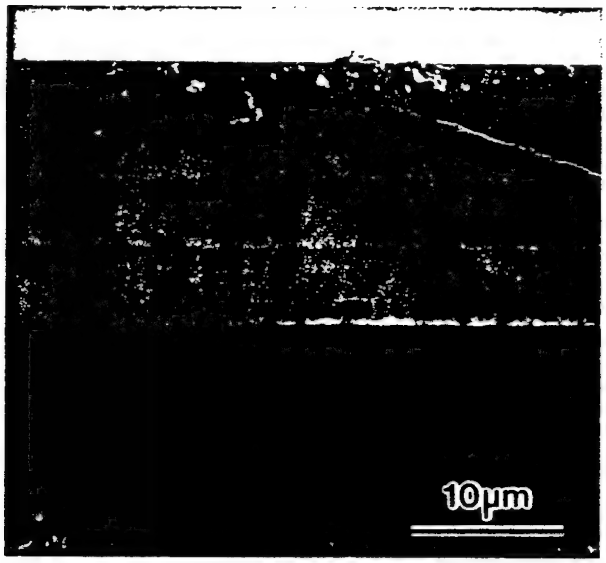

Fig. 3

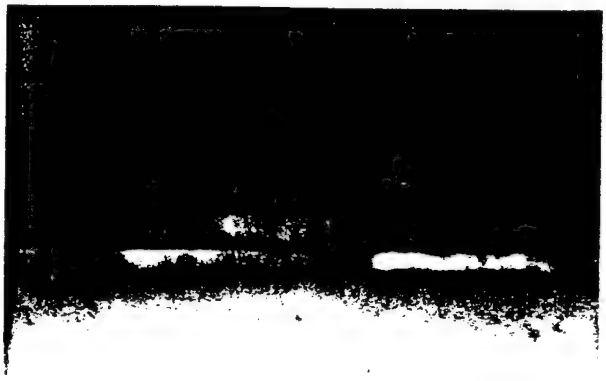

1μm

Fig. 4

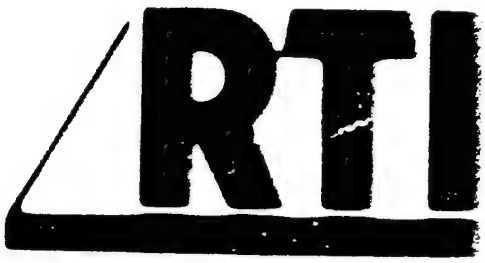

Fig. 5

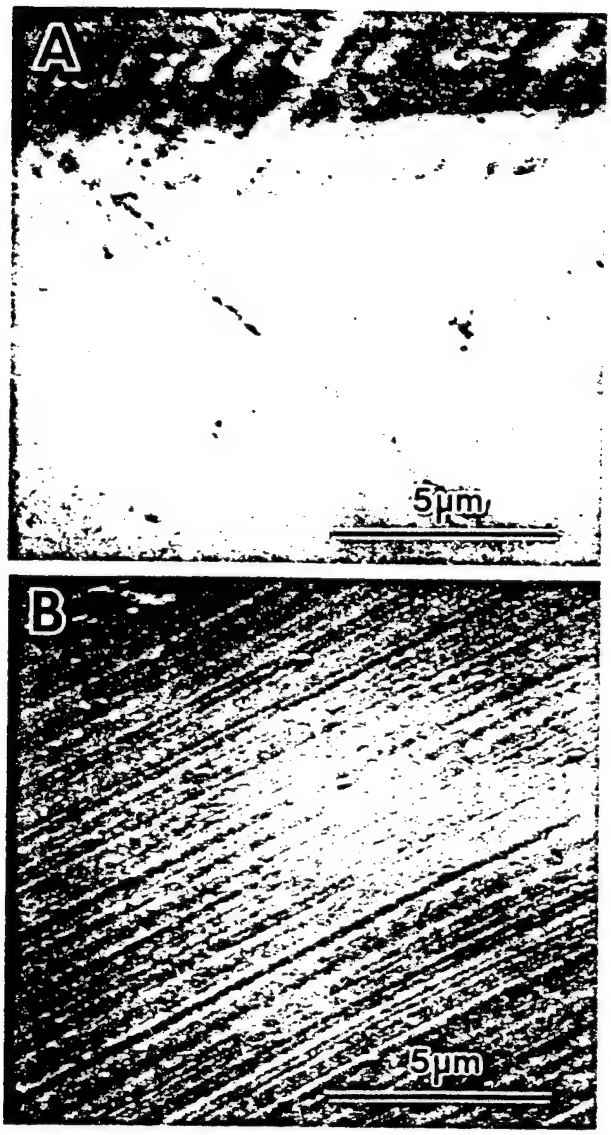

Fig. 6

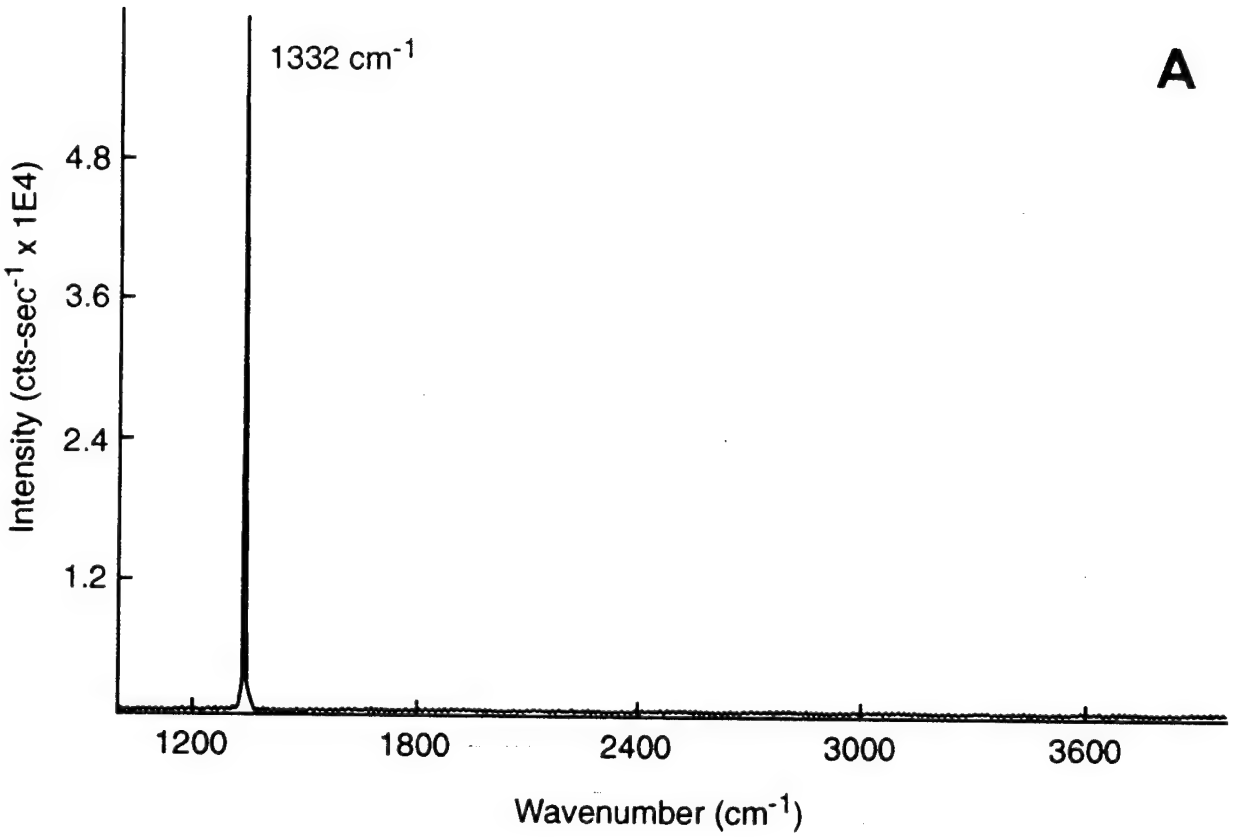
1332 cm-1
A
4.8
3.6
2.4
1.2
Intensity (cts-sec-1 x 1E4)
1200
1800
2400
3000
3600
Wavenumber (cm-1)

Fig. 7A

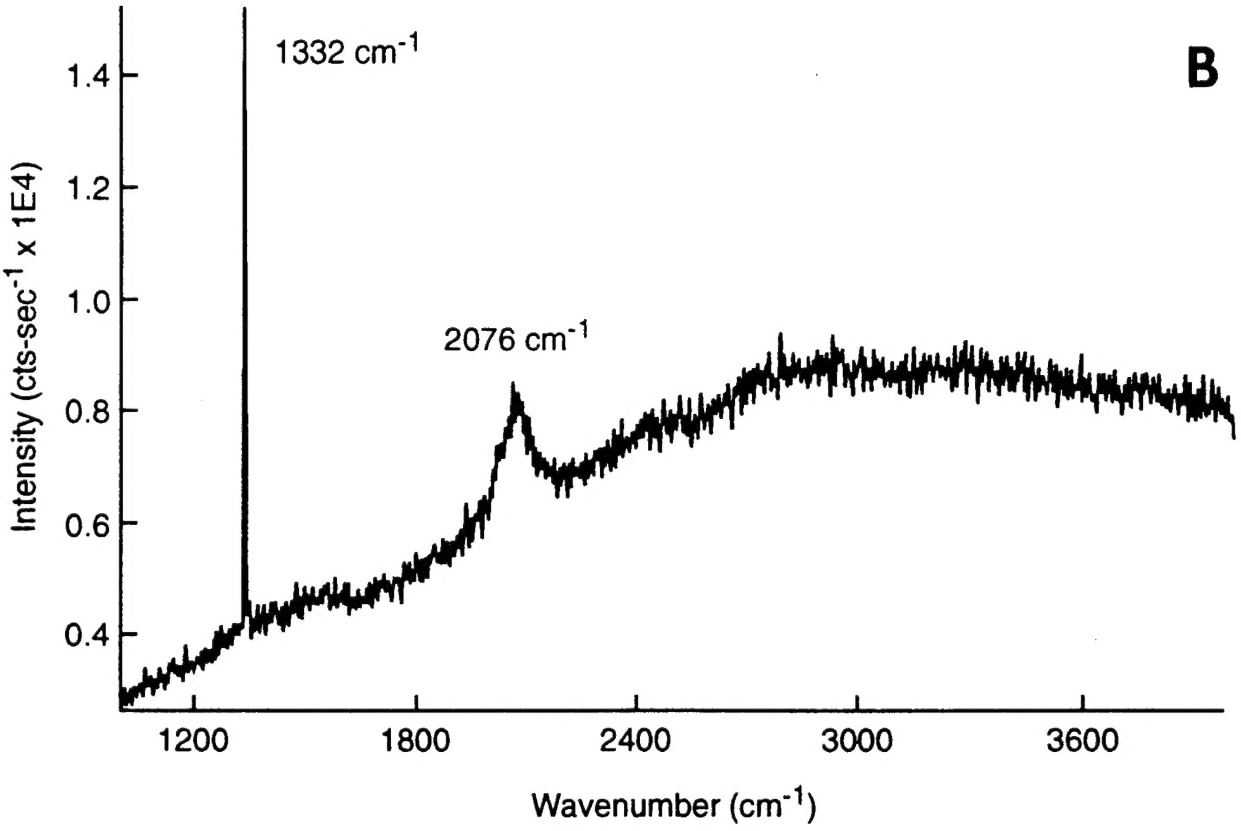
1332 cm-1
B
2076 cm-1
Intensity (cts-sec-1 x 1E4)
1.4
1.2
1.0
0.8
0.6
0.4
1200
1800
2400
3000
3600
Wavenumber (cm-1)

Fig. 7B

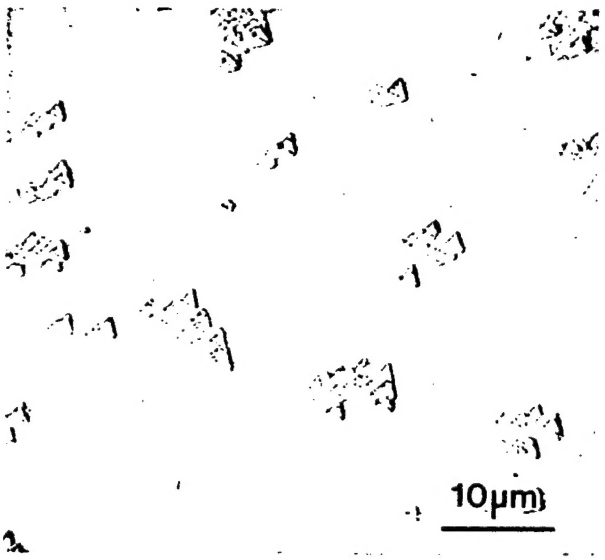

Fig. 8

INTERPRETATION OF SECONDARY ELECTRON CONTRAST FROM NEGATIVE ELECTRON AFFINITY DIAMOND SURFACES

D.P. Malta, J.B. Posthill, T.P. Humphreys, and R.J. Markunas
Research Triangle Institute, Research Triangle Park, North Carolina 27709

Diamond is a wide band-gap semiconductor with many unique physical properties that make it an attractive technological material. One such property is the negative electron affinity (NEA) behavior of the surface when properly terminated with hydrogen[1,2] or a thin metal layer[3]. The NEA diamond surface exhibits an unusually large secondary electron (SE) yield[4] which is desirable for applications in cold cathode electron emitters of flat panel displays. Examination of NEA diamond surfaces by scanning electron microscopy (SEM)[5] has indicated that a unique mechanism appears to be responsible for the SE contrast in which sub-surface microstructural information is contained. This paper provides a brief interpretation of the origin of SE contrast from the NEA diamond surface.

The electron affinity of a semiconductor surface, χ, is defined by the position of the vacuum energy level, E_o, relative to the conduction band minimum, E_c (Fig. 1a). If $\chi>0$, excited conduction band electrons must migrate to the surface and arrive with sufficient kinetic energy to overcome the surface energy barrier in order to escape into vacuum. The probability, p(x), that an electron generated at a depth x will migrate to the surface with sufficient escape energy is:

$$p(x) = C \exp(-x / L_{eff})$$

where C is a constant <1 and L_{eff} is the effective mean escape depth[6]. For χ small and positive, $L_{eff} \approx L_T$, the thermalization length defined as the average distance an excited electron travels before losing excess energy with respect to the conduction band edge. L_{eff} is typically about 0.5-1.5nm in metals and 10-20nm in insulators[7]. For a short L_{eff}, SE contrast originates very near the surface, the effective emission area, d_{eff}, is very small allowing high spatial resolution, and surface topography usually provides the principle source of contrast. Fig. 2a is a SE image of a positive electron affinity "clean" natural diamond surface. Only topographical contrast is observed. For $\chi<0$ (Fig. 1b), the escape depth is no longer limited by the thermalization length since no excess kinetic energy is required to escape the surface. If $\chi<0$, then $L_{eff} \approx L_D$, the diffusion length defined by the average distance a minority free electron can travel before being annihilated by recombination. Since typically, $L_D >> L_T$, the escape depth from the NEA surface is much larger. This results in a higher SE yield, a larger effective escape area, d_{eff}, and poorer spatial resolution. A large component of the total SE signal, I_{SE}, from the NEA surface carries sub-surface information which easily dominates the topographical signal component. If a free electron is generated in the vicinity of a crystalline defect, L_D is considerably shortened, as these defects typically act as free electron traps. Since the intensity of SE emission is proportional to p(x), emission near defects will be suppressed creating defect contrast in SE images of NEA diamond surfaces (Fig. 2b).

The unique SE contrast observed from NEA diamond surfaces is, therefore, attributed to an unusually large effective escape depth for SE electrons resulting from a barrier-free surface condition. The SE signal is dominated by sub-surface information and contrast is provided by microcrystalline defects acting as free electron traps[8].

Microscopy Society of America,
Annual Meeting and Proceedings
1995.

References

1. F.J. Himpsel, J.A. Knapp, J.A. van Vechten and D.E. Eastman, Phys.Rev. B **20**, 624 (1979).

2. B. B. Pate, P.M. Stefan, C. Binns, P.J. Jupiter, M.L. Shek, I. Lindau and W.E. Spicer, J. Vac. Sci. Technology. **19**, 349 (1981).

3. J. van der Weide and R.J. Nemanich, J. Vac. Sci. Technol. B., Vol. 10, 1940 (1992)

4. D.P. Malta, J.B. Posthill, T.P. Humphreys, R.E. Thomas, G.G. Fountain, R.A. Rudder, G.C. Hudson, M.J. Mantini, and R.J. Markunas, Appl. Phys. Lett. **64**, 1929 (1994).

5. D.P. Malta, J.B. Posthill, T.P. Humphreys, R.E. Thomas, R.A. Rudder, G.C. Hudson, M.J. Mantini and R.J. Markunas, Proceedings of the 28th Annual Microbeam Analysis Society Meeting, (Ed. J.J. Friel), July 31-August 5, (1994), 205

6. J. van Laar, Acta Electronica, **16**,3,(1973) 215

7. H. Seiler, Z. Angew Phys. **22** (1967) 249

8. The authors gratefully acknowledge support of this work by BMDO/IST through ONR (Contract No. N00014-92-C-0081) and the helpful assistance of Janice Stephens for manuscript preparation.

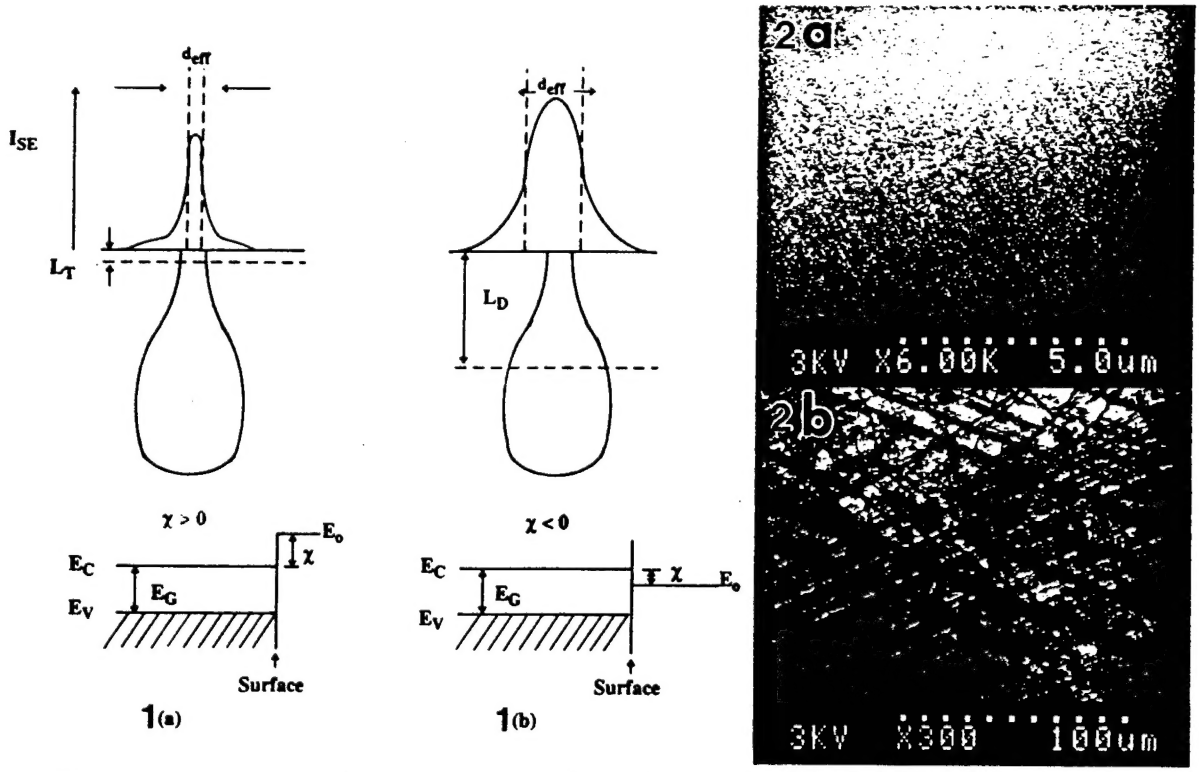

Fig. 1 Schematic diagrams of energy band configurations and origins of secondary electron signal from diamond (a) positive electron affinity surface, (b) negative electron affinity surface.

Fig. 2 Secondary electron images of a polished natural type IIa diamond surface: (a) "clean" surface; $\chi > 0$; topographical polishing scratches observed only; (b) H-terminated surface; $\chi < 0$; defect contrast is observed; surface orientation is (110); defects show directional clustering (diagonal lines) and cellular clustering (dark random lines).